

Shining Light on the Microscopic Resonant Mechanism Responsible for Cavity-Mediated Chemical Reactivity

Christian Schäfer,^{1,2,3,4,*} Johannes Flick,^{5,6,†} Enrico Ronca,^{7,‡} Prineha Narang,^{6,§} and Angel Rubio^{1,2,5,¶}

¹Max Planck Institute for the Structure and Dynamics of Matter and
Center for Free-Electron Laser Science & Department of Physics,
Luruper Chaussee 149, 22761 Hamburg, Germany

²The Hamburg Center for Ultrafast Imaging, Luruper Chaussee 149, 22761 Hamburg, Germany

³Department of Physics, Chalmers University of Technology, 412 96 Göteborg, Sweden

⁴Department of Microtechnology and Nanoscience, MC2,
Chalmers University of Technology, 412 96 Göteborg, Sweden

⁵Center for Computational Quantum Physics, Flatiron Institute, 162 5th Ave., New York, 10010 NY, USA

⁶John A. Paulson School of Engineering and Applied Sciences,
Harvard University, Cambridge, Massachusetts 02138, USA

⁷Istituto per i Processi Chimico Fisici del CNR (IPCF-CNR), Via G. Moruzzi, 1, 56124, Pisa, Italy
(Dated: May 26, 2022)

Strong light-matter interaction in cavity environments is emerging as a promising approach to control chemical reactions in a non-intrusive and efficient manner. The underlying mechanism that distinguishes between steering, accelerating, or decelerating a chemical reaction has, however, remained unclear, hampering progress in this frontier area of research. We leverage quantum-electrodynamical density-functional theory to unveil the microscopic mechanism behind the experimentally observed reduced reaction rate under cavity induced resonant vibrational strong light-matter coupling. We observe multiple resonances and obtain the thus far theoretically elusive but experimentally critical resonant feature for a single strongly-coupled molecule undergoing the reaction. While we do not explicitly account for collective coupling or intermolecular interactions, the qualitative agreement with experimental measurements suggests that our conclusions can be largely abstracted towards the experimental realization. Specifically, we find that the cavity mode acts as mediator between different vibrational modes. In effect, vibrational energy localized in single bonds that are critical for the reaction is redistributed differently which ultimately inhibits the reaction.

In recent years, strong light-matter interaction [1] has experienced a surge of interest in chemistry and material science as a fundamentally new approach for altering chemical reactivity and physical properties in a non-intrusive way [2–6]. Seminal experimental and theoretical work has illustrated the possibility to control photo-chemical reactions [7–12] and energy transfer [13–20], strongly couple single molecules [21–24] or extended systems [25–27]. Vibrational strong-coupling is a particularly striking example. For instance, it was observed that coupling to specific vibrational excitations can inhibit [28–30], steer [31], and even catalyze [32] a chemical process at room temperature. While experimental work continues to make strides, a theoretical understanding of the microscopic mechanism that controls chemical reactions *via* vibrational strong-coupling still remains largely unexplained. Initial attempts to describe vibrational strong-coupling in terms of equilibrium transition-state theory [33–35] have suggested no dependence on the cavity frequency, in stark contrast with the experimental observations. A second approach suggesting an effective dynamical caging by the cavity [36] partially introduced fre-

quency dependence, but so far has been unable to connect to the experimentally observed frequency dependence.

In this work, we report the first comprehensive picture of the microscopic resonant mechanism responsible for cavity-mediated chemical reactivity that qualitatively agrees with the experimental observations [28, 29, 31]. Specifically, we observe the inhibition of the deprotection reaction of 1-phenyl-2-trimethylsilylacetylene (PTA) presented in ref. [28] and schematically illustrated in fig. 1. Our *ab initio* investigations obtain the resonant conditions observed in experiment without the presence of a solvent, thus resolving a recent debate questioning previous experimental investigations [37, 38]. Importantly, our calculations support the hypothesis that coupling vibrational modes involving the reactive atoms modifies the chemical reactivity. This has been partially indicated by experiments [28, 31]. At the same time, we recover critical features of previous theoretical investigations, including the need to go beyond classical transition-state theory and the appearance of dynamical caging effects, which allows to deduce their relevance for experimental realizations. While further investigations will be necessary to entirely resolve the effects behind vibrational strong-coupling, we provide critical theoretical evidence to settle an active debate in the field [28, 33–38], suggesting that strong-coupling to specific vibrational modes can indeed modify chemical reactivity.

Our approach relies on the recently introduced

* Electronic address: christian.schaefer.physics@gmail.com

† Electronic address: jflick@flatironinstitute.org

‡ Electronic address: enrico.ronca@pi.ipcf.cnr.it

§ Electronic address: prineha@seas.harvard.edu

¶ Electronic address: angel.rubio@mpsd.mpg.de

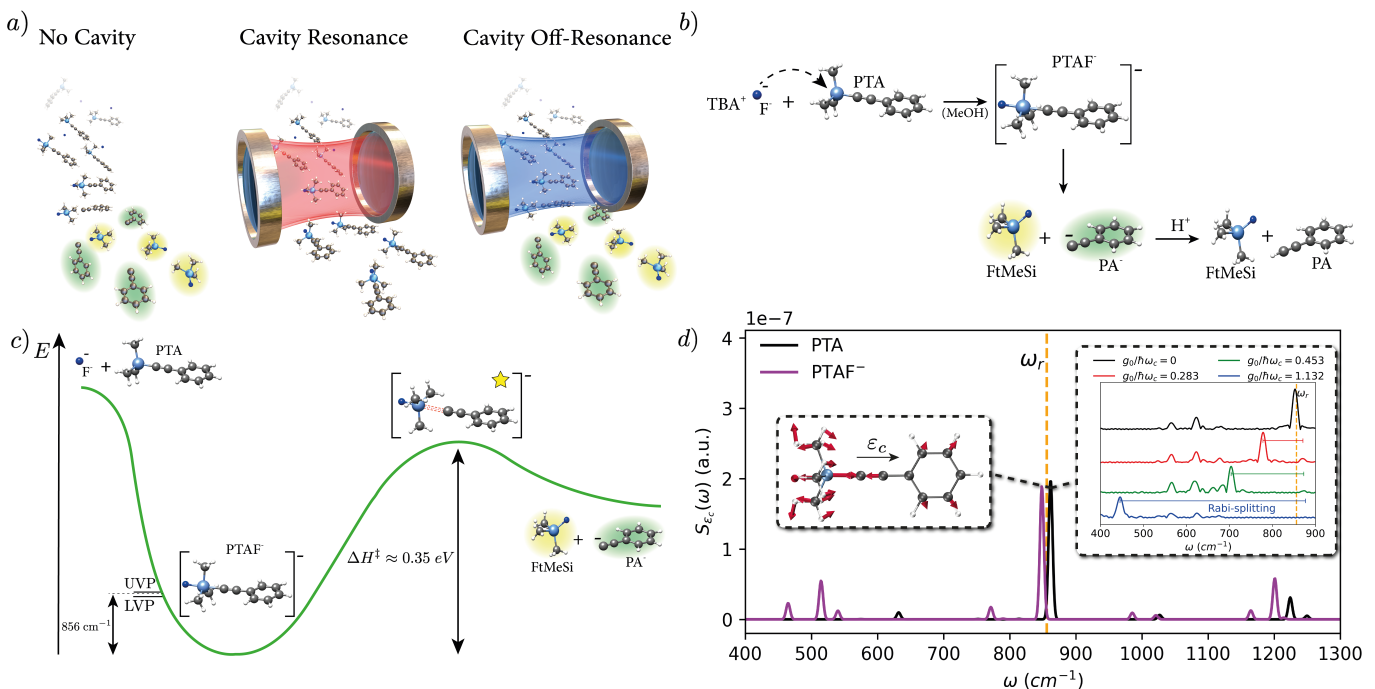


FIG. 1. (a) Resonant vibrational strong-coupling can inhibit chemical reactions. (b) Illustration of the reaction mechanism for the deprotection of 1-phenyl-2-trimethylsilylacetylene (PTA), with tetra-*n*-butylammonium fluoride (TBAF) and (c) energetic of the reaction in (b) in free-space. The successful reaction involves breaking the Si-C bond and thus overcoming a transition-state barrier of 0.35eV. (d) Vibrational absorption spectrum along the cavity polarization direction $S_e(\omega) = 2\omega \sum_{j=1}^{N_{vib}} |\epsilon_c \cdot \mathbf{R}(\omega_j)|^2 \delta(\omega - \omega_j)$ illustrating the strong-coupling of the vibrational eigenmode at 856 cm^{-1} with the cavity polarized along ϵ_c for PTAF⁻ (magenta) and the isolated PTA complex (black). The insets show the coupled vibrational mode of PTA and the light-matter hybridization under vibrational strong-coupling. Our time-dependent calculations describe the correlated (non-adiabatic) movement of electrons, nuclei and cavity field during the reaction. The strong asymmetry between lower and upper polariton originates from the high coupling and the related interplay of electronic, nuclear and self-polarization contribution (see SI fig. 2). The cavity frequency will be changed between 43 and 1584 cm^{-1} in order to investigate resonant effects.

quantum-electrodynamical density-functional theory (QEDFT) framework [23, 39–41] that enables the full description of electronic, nuclear and photonic degrees of freedom from first principles. QEDFT recovers the resonant dynamic nature of the chemical inhibition under vibrational strong-coupling, illustrating the strength embodied by first-principle approaches in this context. We find that the cavity introduces a new pathway to redistribute vibrational energy during the reaction. Energy deposited in a single bond during the reaction quickly spreads to the set of correlated modes such that the probability to break a specific bond is diminished. Consequentially, if the coupled mode possesses a substantial Si-C stretching character, relevant in the dissociation step, the reactivity is inhibited.

I. REACTION MECHANISM AND RESONANT VIBRATIONAL STRONG-COUPLING FROM FIRST-PRINCIPLES

Under typical reaction conditions, that is, no vibrational strong-coupling, the deprotection reaction of 1-phenyl-2-trimethylsilylacetylene (PTA) with tetra-

butylammonium fluoride (TBAF) to give phenylacetylene (PA) and fluorotrimethylsilane (FtMeSi) is expected to evolve (see fig. 1 b) as follows [28, 42]. In solution (usually methanol) the F⁻ ions released by TBAF form an intermediate pentavalent complex (PTAF⁻) that reduces considerably the barrier for the dissociation of the Si-C bond, inducing the exit of the phenylacetylide anion (PA⁻). In solution a fast protonation of the PA⁻ brings to the formation of the final phenylacetylide (PA) product. Here, we will describe the explicit evolution of the reaction for a single molecule represented by an ensemble of thermally distributed independent trajectories that follow the equations of motion provided by (quantum-electrodynamical) density-functional theory. Our numerical investigations start from the PTA+F⁻ initial state over the intermediate pentavalent PTAF⁻ complex up to the breaking of the Si-C bond (see fig. 1 c), thus explicitly including the rate limiting step (PTA+F⁻ → FtMeSi + PA⁻).

In order to simulate vibrational strong coupling inside the cavity and its effect on the reaction, we couple a single cavity mode with variable frequency ω_c , effective cavity volume V_c , and fixed polarization ϵ_c to the

molecular dipole moment $\hat{\mathbf{R}}$ according to $\hat{H} = \hat{H}_{\text{Matter}} + \hbar\omega_c(\hat{a}^\dagger\hat{a} + \frac{1}{2}) + \sqrt{\frac{\hbar\omega_c}{2\varepsilon_0V_c}}(\boldsymbol{\varepsilon}_c \cdot \hat{\mathbf{R}})(\hat{a}^\dagger + \hat{a}) + \frac{1}{2\varepsilon_0V_c}(\boldsymbol{\varepsilon}_c \cdot \hat{\mathbf{R}})^2$ [40, 43]. The dimensionless ratio $g_0/\hbar\omega_c$ with coupling $g_0 = ea_0\sqrt{\hbar\omega_c/2\varepsilon_0V_c}$ provides an indication for relative light-matter coupling strengths. In order to limit the considerable computational cost of our calculations, we will focus in the following on a subset of quickly reacting trajectories (details in Materials and Methods IV). This preferential selection implies that the cavity has to exert sizeable effects on the single molecule within a short time-frame. Since this timescale is correlated with the light-matter coupling strength, we require also a sizeable (enhanced) light-matter coupling strength in our simulations. Increasing the coupling strength further inhibits the chemical reaction (see SI), we observe the same trend as in experiment [28]. The specific value chosen here does not influence the qualitative observation, as discussed in the SI, but dominantly determines the strength of the influence of the cavity on the reaction. We will discuss in the following how such local effective couplings could emerge and their relation to experiment. Retaining the quadratic operator (self-polarization) $\frac{1}{2\varepsilon_0V_c}(\boldsymbol{\varepsilon}_c \cdot \hat{\mathbf{R}})^2$ is critical to ensure a physically sound result [43]. The correlated evolution of electronic, nuclear, and photonic system is described by quantum-electrodynamical density-functional theory using Ehrenfest’s equation of motion for nuclear and Maxwell’s equation for photonic degrees of freedom [40] (details in Materials and Methods IV).

A prerequisite for reactive control is the strong-coupling condition, that is, a hybridization energy between vibration and cavity larger than the combined decoherence of the system. Intuitively, the cavity excitation would be overlaid with a vibrational excitation and the hybridization correspondingly becomes visible. Obtaining vibro-polaritonic spectra and confirming the strong-coupling condition is thus a first essential step in any *ab initio* QED chemistry investigation. Fig. 1 d illustrates a subset of the vibrational absorption spectrum along the cavity polarization axis for isolated PTA and pentavalent PTAF⁻ complex. A clear vibrational resonances is observed around $\omega_r = 856 \text{ cm}^{-1}$, suggesting that the vibrational strong-coupling conditions are met around the local minimum (PTAF⁻) as well as for all molecules previous to any reaction (PTA). Surely, many other vibrational resonances are available.

During the reaction, however, the molecular geometry and consequently its vibrational spectrum change considerably (more details in the SI) such that simulations involving a single molecule are unlikely to exhibit a sharp resonant condition for an effect of the cavity on the reaction. In addition, the Si-C bond of special interest contributes to a set of vibrational eigenmodes which are distributed over a wide frequency-range. In combination, retaining exact resonance between a specific cavity mode and a specific vibrational mode during the reaction is virtually impossible but also not necessary. Our investigations illustrate that reduced model descriptions, while

powerful and intuitive in many situations, can be misleading at times and that first principles calculations are essential in the future understanding and development of polaritonic chemistry.

II. CAVITY INDUCED INHIBITION OF A GROUND-STATE CHEMICAL REACTION

In order to identify the physical microscopic mechanism behind the cavity induced inhibition of the Si-C bond-breaking, we perform extensive real-time quantum-electrodynamical density-functional theory calculations for a set of 30 trajectories which are launched with initial conditions sampled from a thermal distribution at 300 Kelvin. A subset of 8 trajectories undergoing the reaction outside the cavity will be used for all further analysis. The high computational cost of the current framework limits the number of trajectories that we can address in the statistical ensemble. This demands to sample more densely around highly reactive trajectories which shortens the average reaction-speed. As a consequence, the light-matter coupling strength is artificially increased to enhance cavity-mediated phenomena at those shorter time-scales. Smaller coupling values provide similar predictions (see SI) but would require more computational resources to resolve the cavity influence. The subsequent investigations provide thus strong indications of cavity modified reactivity but are certainly limited in their statistical significance. Fig. 2 illustrates one such exemplary trajectory in free-space (black), inside a off-resonant cavity (red) and when strongly coupled to the resonant cavity-mode (orange). The potential energy surface is shown here for illustrative purposes only and has not been employed in the propagation. For the given set-up, the way F⁻ attaches and how the pentavalent PTAF⁻ complex is formed is barely disturbed. Once the molecule enters the pentavalent complex, a clear change in the dynamics of the Si-C bond is observed in resonance. The resonant cavity effectively traps the system around the local minimum, extending the reaction-time beyond the simulation time of 1 ps by protecting the Si-C bond from dissociating.

To further elucidate the bond-strengthening feature of the cavity, we project the dynamical nuclear coordinates during the time-dependent evolution on the vibrational eigenmodes of the bare PTAF⁻ system (without cavity). Fig. 3 shows the difference of mode occupation between strong resonant coupling $\omega_c = 856 \text{ cm}^{-1}$ and far off-resonant coupling $\omega_c = 43 \text{ cm}^{-1}$. Particularly relevant is the time-domain in which the F anion attaches to PTA at 200 fs and the Si-C bond-breaking in free-space at 500 fs. Without surprise, many (anharmonic) vibrational modes contribute to the reaction, rendering it challenging to describe the reaction in terms of a reduced subset of coordinates. While the cavity has an overall minor effect on the vibrational occupations, it leads to considerable redistribution of occupation in modes along the F-

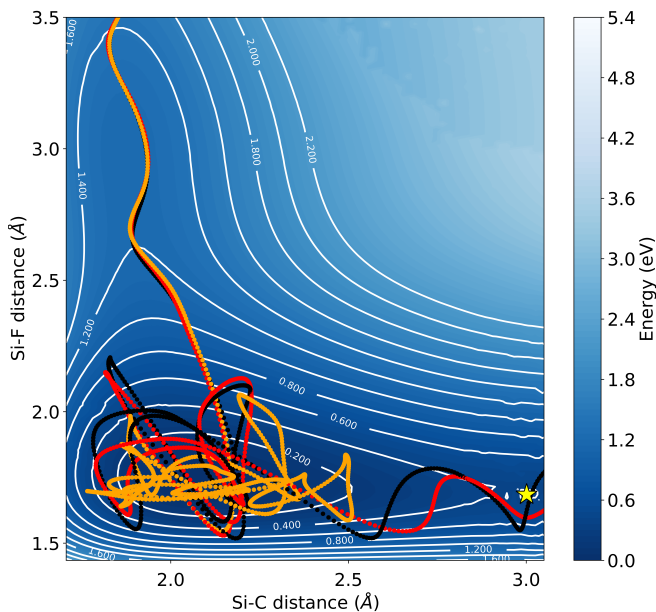


FIG. 2. Exemplary trajectory outside $g_0/\hbar\omega_c = 0$ (black), inside the cavity on resonance $g_0/\hbar\omega_c = 1.132$, $\omega_c = 856 \text{ cm}^{-1}$ (orange) and off-resonant $g_0/\hbar\omega_c = 1.132$, $\omega_c = 1712 \text{ cm}^{-1}$ (red) undergoing the reaction illustrated in fig. 1 (b, c). The transition-state is indicated with a yellow star. Encoded in the transparency is the relative angle between Si-C and cavity polarization axis (inset fig. 1 d). The molecular axis remains largely oriented along the cavity polarization during the reaction.

Si-C-C chain. For instance, between 240 and 310 fs, the cavity mode induces a coherent exchange of occupation between the coupled mode at 849 cm^{-1} and the vibration at 540 cm^{-1} . This coherent exchange seems to originate from the structural similarity between the involved vibrational modes, both featuring strong methyl and Si-F contributions. Si-F and Si-C bond are correlated with a strength that is slightly decreasing under resonant light-matter coupling (see SI fig. 5). Interestingly, the strongest changes appear for the modes at 771 , 515 and 465 cm^{-1} , all characterized by strong F-Si-C contributions and with minor or no methyl contribution. Resonant coupling between cavity and the mode at 849 cm^{-1} is thus altering foremost the energy exchange within the F-Si-C-C bond-chain. To summarize, the cavity can prevent the bond-breaking of Si-C by redistributing energy into other vibrations along the F-Si-C-C chain. This effectively correlates the vibrations along the chain protecting the Si-C bond. The dominant effect of vibrational strong coupling on a ground-state chemical reaction would be therefore that it provides means to alter the redistribution of energy from a specific bond into other degrees of freedom. Particularly relevant for this mechanism is the Si-C character of the coupled vibration as will be shown in the following. These observations suggest a clear dependence on the symmetry of the molecule and associated reaction pathways, in conceptually close agreement with recent experimental investigations [44]. We note that, we

decided here to compare between resonant cavity and strongly detuned cavity in order to eliminate the potential influence of self-polarization contributions that are frequency independent and become relevant in the ultra-strong coupling domain (see e.g. SI fig. 2).

We acknowledge that such correlations *via* the cavity-mode would necessarily depend on the specific chemical complex, reaction mechanism and ambient conditions. Our results and experimental observations [28, 29, 31] suggest, however, that tuning the cavity in resonance to a molecular vibrational excitation with relevant contribution to reactive bonds prefers to inhibit typically dominant reaction pathways. In our investigations, the inhibition of the reaction for a given temperature can be overcome by increasing the molecular temperature to the point that the energetic redistribution mediated by the cavity becomes negligible. Each pathway affected by the cavity becomes increasingly sensitive to thermal changes. This provides room for other usually suppressed pathways, leads to an overall tilt in the reactive landscape, and alters the thermodynamic characteristics of the reaction. Whether catalytic effects *via* vibrational strong-coupling to solvents [32] follow the same rationale and pathway remains an open question.

The experimental conditions in references [28, 29, 31, 32] suggest an involvement of a macroscopic number of molecules N that collectively couple to the cavity excitation, effectively representing a set of synchronized oscillators leading to a \sqrt{N} enhancement of the effect. Such a collective interaction clearly shows up in an optical measurement but it does not necessarily imply that a single molecule is strongly affected by the light-matter interaction as the local contribution in a collective state will scale with $1/\sqrt{N}$. However, the individual molecule undergoing the reaction will continuously change its vibrational structure and no longer behave as the large ensemble of identical collectively coupled reactant molecules. This might call for the introduction of a more local interpretation of collective strong coupling in chemistry. Indeed, recent theoretical work suggests that Coulomb mediated correlations and collective strong coupling can lead to local strong coupling for a molecular impurity as the individual molecule can experience a collectively enhanced dipole moment [5, 45, 46]. It is important to realize that such an amplification of the dipole coupling for the impurity molecule still depends on the strong coupling and the resonant condition of the whole ensemble. The sensitivity of the ensemble strong coupling is enforced onto the single molecule strong coupling via this amplification effect. In this work we focus on the single-molecular strong coupling and acknowledge that the precise interplay between collective ensemble and local chemistry represents an open problem in the field. In addition to the here observed intramolecular energy redistribution, intermolecular interactions mediated by the cavity might further inhibit accumulation of energy in specific bonds, thus preventing specific reactions. Recent molecular-dynamics force-field simulations address-

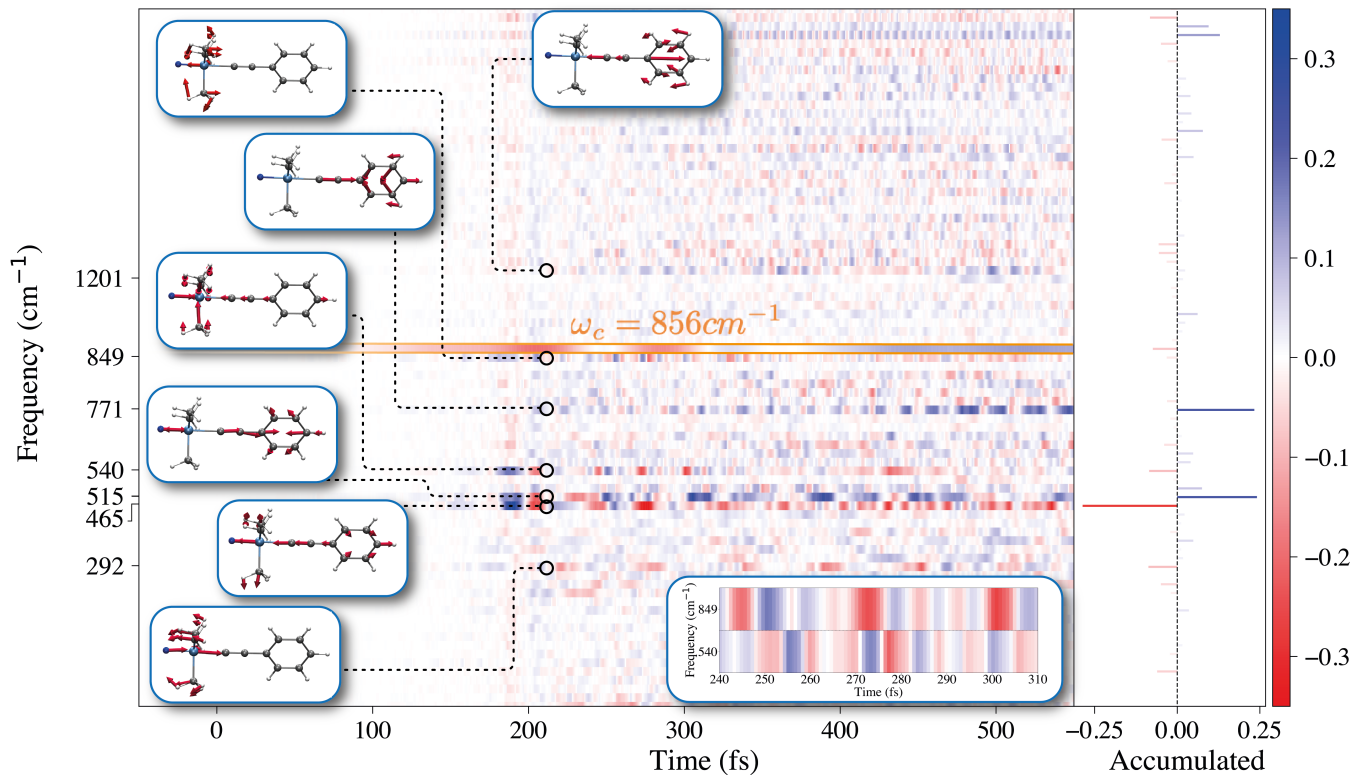


FIG. 3. Time-resolved influence on the mode occupations by resonant vibrational strong-coupling. Illustrated is the trajectory averaged difference in normalized mode-occupation between on resonant condition $\omega_c = \omega_r = 856 \text{ cm}^{-1}$, $g_0/\hbar\omega_c = 1.132$ and far off-resonance $\omega_c = 43 \text{ cm}^{-1}$, $g_0/\hbar\omega_c = 1.132$ for all 8 trajectories that undergo the reaction outside the cavity. The bar-plot shows the accumulated difference divided by a factor of 100. The cavity mode (bordered orange) is here represented by the difference in normalized mode-displacement $q(t) = \sqrt{\hbar/2\omega_c}(\hat{a}^\dagger + \hat{a})$ and re-scaled by the factor 1/4. Insets illustrate relevant normal modes or highlight the correlated occupancy between modes 849 and 540 cm^{-1} .

ing the energetic relaxation of CO_2 molecules suggest indeed that the cavity can facilitate intermolecular redistribution of vibrational energy [20]. Experimental ambient conditions influence the coherence of those processes and will likely determine the relevance of intra- and intermolecular vibrational energy redistribution. Further, intra- and intermolecular processes should obey a different dependence on the symmetry of the molecule. The combination of both ‘handles’ could provide a possible path to elucidate their individual relevance in vibrational strong-coupling.

A. Observation of a Resonant Effect

While experiments so far have indicated a clear dependence on the resonant conditions between vibration of interest and the cavity mode, theory has not been able to agree with this as a critical prerequisite. Hidden in the overall debate are two aspects that are combined in a single experimental observation. The first is the strong-coupling condition itself. When decoherences are stronger than the light-matter interaction no hybridization and subsequently no relevant effect on the chemical reaction

can be observed [28]. Second, the vibrations that dominantly contribute to the bond-breaking have to be involved in this strong-coupling condition.

In our *ab initio* theoretical investigation, the strong-coupling condition is always fulfilled, and thus we dominantly investigate the second resonant condition. By varying the length of the idealized Fabry-Pèrot cavity, we tune the frequency of the cavity mode while keeping the ratio between coupling and frequency $g_0/\hbar\omega_c$ constant. Fig. 4 illustrates our extensive *ab initio* calculations addressing the resonant effect in a compact trajectory averaged form. We show the trajectory averaged Si-C distance over time (a), the time-averaged Si-C distance (b), the spectrum along the cavity polarization of PTAF^- and the spectrum weighted with its Si-C contribution (c).

All trajectories that undergo the reaction outside the cavity (dotted black lines) show a diminished reactivity inside the cavity. Clear resonant features appear around 86 (red dashed-dotted vertical line), 290, 570 and 1300 cm^{-1} in addition to a broad shoulder between 600 and 1000 cm^{-1} that includes the experimentally investigated resonance at 856 cm^{-1} (orange dashed vertical line). Setting fig. 4 (b) in relation to the vibrational spectrum in fig. 4 (c) illustrates two different mechanisms. At 86 cm^{-1}

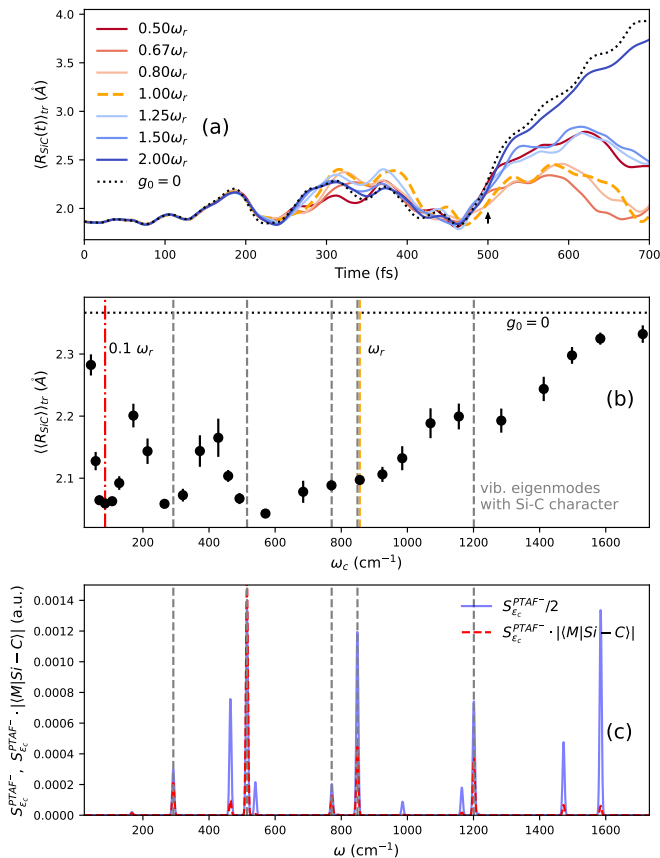


FIG. 4. Time-resolved trajectory averaged Si-C distance (a), time-averaged Si-C distance $\langle\langle R_{SiC} \rangle\rangle_{tr}$ (b), and (Si-C weighted) spectral strength in polarization direction (c) for varying cavity frequency ω_c relative to the resonant frequency $\omega_c = \omega_r = 856 \text{ cm}^{-1}$. The ratio $g_0/\hbar\omega_c = 1.132$ is kept constant. Error-bars show the standard error of the trajectory average. We use all 8 trajectories that show the reaction outside the cavity. In free-space (black dotted), the reactive trajectories will start to break the Si-C bond at around 500 fs (indicated by the black arrow). The cavity has the overall tendency to prevent the formerly reactive trajectories from breaking the Si-C bond. This effect shows a complex frequency dependence that includes two separate regimes as explained in the text. The Si-C-stretching weight $|M|Si - C|$ was obtained by projecting the normalized Si-C stretching on the vibrational modes.

(red dashed-dotted vertical line), no vibrational spectral density exists but the energy coincides with the curvature of the potential energy surface at the transition-state (see SI). This leads to a dynamical caging effect of the trajectory around the transition-state, in agreement with recent findings by Li et al. [36] and discussed in more detail in the SI, that prevents the chemical reaction. No experiment investigated this frequency domain so far such that this mechanism seems unrelated to the experimental realizations. The lack of vibrational spectral density in this domain would prevent the occurrence of polaronic states. The second mechanism involves all vibrational modes with a sizeable Si-C-stretching contribution (c, red dashed line), indicated by grey-dashed vertical

lines in (b) and (c). Comparison with fig. 3 clarifies that the highlighted vibrational modes play a central role in the reaction mechanism and are strongly affected by the cavity. Intuitively, stronger Si-C character in the polaronic states will affect the Si-C bond stronger, resulting in the proposed mechanism of a cavity induced vibrational energy redistribution that effectively strengthens the Si-C bond and prevents the reaction. Maximising the light-matter coupling strength via large spectral weight and ensuring a high Si-C character suggests the vibration at 515 cm^{-1} as most promising. The corresponding mode projection is illustrated in the SI Fig. S5. It should be acknowledged however that we find especially the spectral intensity to be sensitive to approximations in the theoretical description (see SI). Larger frequencies imply larger fundamental couplings which in turn result in a stronger contribution of the self-polarization reflecting in an increased blue-shift (see SI).

The experimental counterpart focused on a small frequency domain around the 856 cm^{-1} vibration [28]. A subsequent publication investigating the influence of collective strong coupling on silyl cleavage reactions for a related structure [31] identified however a clear effect of the cavity when tuned to one out of three vibrations located at 842, 1110 and 1250 cm^{-1} . This supports our hypothesis and suggests that vibrational strong coupling could represent an even more flexible tool for chemistry than currently hoped. A noticeable difference between our theoretical calculations and experiments is the broadness of the observed resonant features. As in the present work, we are computationally limited to a single molecule and a small set of trajectories. Energy redistribution can appear then only between modes in the same molecule (intramolecular energy redistribution). When larger ensembles of molecules collectively couple to the cavity intermolecular energy redistribution will likely provide additional and potentially more efficient channels for energy redistribution. In order to observe a significant effect for a small set of trajectories it was necessary to select quickly reacting initial configurations and large light-matter couplings. The corresponding short reaction times and large couplings lead to an influence of the cavity on much shorter time-frames than in experiments and suggest therefore broader frequency features than in experiment. Nevertheless, the qualitative agreement between the here observed mechanism and the experimentally observed features suggests that the here proposed mechanism, i.e., vibrational strong-coupling mediated energy redistribution and subsequent protection of the Si-C bond, largely explains the experimentally observed chemical effect.

III. CONCLUSIONS AND OUTLOOK

Strong light-matter coupling in cavity environments provides a conceptually new and potentially invaluable addition to the current chemical toolbox [2–4]. By lever-

aging the QEDFT framework, we provide key theoretical insight from first-principles into the inhibition of ground-state reactions under vibrational strong-coupling. Despite disregarding the quantum nature of photons and considering only a single molecule, our results are in good qualitative agreement with experimental observations [28, 29, 31], suggesting that cavity-mediated chemical reactivity can be largely explained by strong classical light-matter interactions. To the best of our knowledge, we present for the first time the ‘in experiment’ observed resonant condition.

During the reaction, energy is accumulated in specific bonds which in free-space lead to their dissociation. Under strong vibrational coupling, the cavity-correlated vibrations redistribute energy differently than in free-space, effectively strengthening the here relevant Si-C bond and ultimately inhibiting the reaction. The cavity serves as mediator to other vibrations, in combination, they represent a strongly frequency dependent bath. Increasing light-matter coupling strength enhances the inhibiting effect of the cavity, we observe a similar trend as in experiment [28]. The resonant condition associated with this microscopic mechanism is apparent and suggests that future theoretical models should focus on an appropriate description of such a frequency dependent bath. Furthermore, our results suggest a sizeable cavity-mediated influence on chemical reactions can be expected when the coupled vibrational mode provides a large oscillator strength and at the same time contributes noticeably to the reaction. Within the here investigated chemical reaction, the cavity provides a way to selectively cool specific vibrations. Recent experiments in which the solvent is strongly coupled [32] suggested that this bath could similarly serve as reservoir, meaning hot solvent molecules transfer energy to the reactant, catalysing the reaction. Our observations are in line with the experimentally observed relevance of the symmetry of the coupled vibrational mode [44] as the energy redistribution between vibrations due to the cavity demands a consistent alignment between vibration and cavity polarization, suggesting that different symmetries will give rise to different reshuffling of energy. Even in absence of collective effects we recover the sought resonant conditions [28, 29, 31]. While intermolecular interactions could contribute to the energy redistribution responsible for the cavity mediated effect on chemical reactivity, the agreement between our theoretical predictions and experimental observations suggests that the mechanism will remain qualitatively similar. It seems however likely that intermolecular energy redistribution could enhance the influence of the cavity. Our observation serves as primer for the understanding of the local microscopic changes in chemical reactions induced by strong light-matter coupling in cavities. Future investigations will explore in more detail how collective effects can modify our conclusions.

In agreement with previous studies [33–36], we conclude that dynamic features play a much more pro-

nounced role under strong light-matter coupling than commonly assumed by standard transition-state-theory for ground-state chemical reactivity. Our *ab initio* description of matter is parameter-free and thus suggests that our conclusions can be extrapolated to similar reactions, providing a precursor to a new field of theoretical *ab initio* polaritonic chemistry. Handles such as symmetry and coherence could elucidate to which extend inter- and intramolecular energy redistribution contribute to vibrational strong-coupling. How such kinetically driven effects can persist into the realm of realistic ambient conditions for large ensembles of reacting molecules thus remains a key question necessitating further theoretical and experimental investigations where the present findings provide the seed to guide them.

IV. MATERIALS AND METHODS

The potential energy surface is obtained using the ORCA code [47] with the 6-31G* basis set, employing DFT and the PBE functional. The time-dependent calculations were performed using the real-space TDDFT code Octopus [48]. Building the pentavalent complex is entropically unfavored and unlikely such that just a very limited set of trajectories would result in a successful attachment of the F anion. To reduce the amount of non-reactive trajectories we kicked the complex out of its local minimum in the pentavalent configuration along the minimal energy path running the reaction backwards towards the initial condition to estimate the collision speed and angle leading to the reaction. We obtained ideal angles between Si-C and Si-F bond of around 180 degrees. An alternative angle for F⁻ to attack Si is at 60 degrees but the latter demands higher temperatures on the order of 900K. Using the linear configuration, we obtained first initial geometries from Orca with a subsequent further optimization in the Octopus code using a constrained force minimization for a fixed Si-F distance of 4 Å. According to fig. 1 of the main text, the initial F⁻+PTA configuration is energetically higher than the transition-state barrier of 0.35 eV such that a few trajectories will undergo the reaction within a reasonable time-frame while the majority will remain trapped in the local minimum of the PTAF⁻ configuration. Starting from those initial geometries, we sample initial velocities according to a Boltzmann distribution at 300 K, i.e., a Gaussian normal distribution with nuclei specific variance $\sigma_{v_i} = \sqrt{k_b T / M_i}$. Furthermore, we point the F momentum towards the Si and remove the center of mass movement. We propagate 10 such trajectories and obtain a single reactive trajectory at 300K shown in fig. 2. Then, in order to limit the necessary number of trajectories while still obtaining a reasonable number of reactive trajectories, we sample around the first reactive trajectory a set of 20 additional trajectories with a relative temperature of 20K, removing again the center-of-mass momentum. We find in total 8 reactive trajectories outside the cavity. If not further speci-

fied the illustrated observables represent the average of those 8 trajectories. Inside the cavity, the initial photon-mode displacement is provided by the zero-electric field condition $q(t_0) = -\frac{\lambda}{\omega} \cdot \mathbf{R} \leftrightarrow \mathbf{E}(t_0) = 0$ with $\dot{q}(t_0) = 0$ and $\mathbf{R} = \sum_i^{N_n} Z_i \mathbf{R}_i - \sum_i^{N_e} \mathbf{r}_i$ [40, 43, 49]. The polarization of the cavity was chosen along the Si-C axis which coincides with the x-axis. This initial configuration is then propagated in the Octopus code [48] using the enforced time-reversal symmetry (electronic subspace) + velocity verlet (nuclear subspace) time-stepping routine with electronic $\Delta t_e = 0.0012/eV$, photonic $\Delta t_p = 10\Delta t_e$ and nuclear $\Delta t_n = 10\Delta t_e$ timesteps. Photonic and nuclear coordinates are accelerated by a factor 10 [40, 50] in order to shorten the calculation time. For the electronic subspace, we use the revPBE [51] electronic exchange and correlation potential and the standard SG15 Pseudo-potential set. The nuclear coordinates are moving according to the classical Ehrenfest equations of motion,

i.e., electronic and nuclear system are self-consistently exerting forces on each other. The photonic coordinates are coupled via the classical Ehrenfest light-matter coupling using the QEDFT framework which leads to classical cavity fields acting on nuclear and electronic degrees of freedom [23, 39–41]. We use a numerical box of $V = (24 a_0)^3$ and a grid spacing of $0.24 a_0$ with the bohr radius a_0 . The parameters of the grid are chosen such that numerically caused changes in the energy are minor compared to thermal energies. We monitor the time-evolution of the complex and define the Si-C bond as broken when the Si-C distance increases beyond the transition-state. The spectra showing the Rabi-splitting in fig. 1 (d) have been obtained by propagating for 3 ps on a grid that combines spheres of size 6 \AA around each atom with a grid spacing of $0.24 a_0$. Here, the nuclei are initialized with random velocities corresponding to 50 K.

-
- [1] S. Haroche and J.-M. Raimond, *Exploring the quantum: atoms, cavities, and photons* (Oxford university press, 2006).
- [2] C. Genet, J. Faist, and T. W. Ebbesen, Inducing new material properties with hybrid light–matter states, *Physics Today* **74**, 42 (2021).
- [3] F. J. Garcia-Vidal, C. Ciuti, and T. W. Ebbesen, Manipulating matter by strong coupling to vacuum fields, *Science* **373** (2021).
- [4] B. S. Simpkins, A. D. Dunkelberger, and J. C. Owrutsky, Mode-specific chemistry through vibrational strong coupling (or a wish come true), *The Journal of Physical Chemistry C* **125**, 19081 (2021).
- [5] D. Sidler, M. Ruggenthaler, C. Schäfer, E. Ronca, and A. Rubio, A perspective on ab initio modeling of polaritonic chemistry: The role of non-equilibrium effects and quantum collectivity (2021), [arXiv:2108.12244 \[physics.chem-ph\]](https://arxiv.org/abs/2108.12244).
- [6] M. Ruggenthaler, N. Tancogne-Dejean, J. Flick, H. Appel, and A. Rubio, From a quantum-electrodynamical light–matter description to novel spectroscopies, *Nature Reviews Chemistry* **2**, 0118 (2018).
- [7] J. A. Hutchison, T. Schwartz, C. Genet, E. Devaux, and T. W. Ebbesen, Modifying chemical landscapes by coupling to vacuum fields, *Angewandte Chemie International Edition* **51**, 1592 (2012).
- [8] B. Munkhbat, M. Wersäll, D. G. Baranov, T. J. Antosiewicz, and T. Shegai, Suppression of photo-oxidation of organic chromophores by strong coupling to plasmonic nanoantennas, *Science Advances* **4**, eaas9552 (2018).
- [9] J. Galego, F. J. Garcia-Vidal, and J. Faist, Suppressing photochemical reactions with quantized light fields, *Nature Communications* **7**, 13841 (2016).
- [10] M. Kowalewski, K. Bennett, and S. Mukamel, Cavity femtochemistry: Manipulating nonadiabatic dynamics at avoided crossings, *The journal of physical chemistry letters* **7**, 2050 (2016).
- [11] G. Groenhof, C. Climent, J. Faist, D. Morozov, and J. J. Toppari, Tracking polariton relaxation with multiscale molecular dynamics simulations, *The journal of physical chemistry letters* **10**, 5476 (2019).
- [12] J. Fregoni, G. Granucci, M. Persico, and S. Corni, Strong coupling with light enhances the photoisomerization quantum yield of azobenzene, *Chem* **6**, 250 (2020).
- [13] D. M. Coles, N. Somaschi, P. Michetti, C. Clark, P. G. Lagoudakis, P. G. Savvidis, and D. G. Lidzey, Polariton-mediated energy transfer between organic dyes in a strongly coupled optical microcavity, *Nature Materials* **13**, 712 (2014).
- [14] E. Orgiu, J. George, J. A. Hutchison, E. Devaux, J. F. Dayen, B. Doudin, F. Stellacci, C. Genet, J. Schachenmayer, C. Genes, G. Pupillo, P. Samorì, and T. W. Ebbesen, Conductivity in organic semiconductors hybridized with the vacuum field, *Nat. Mater.* **14**, 1123 (2015).
- [15] X. Zhong, T. Chervy, S. Wang, J. George, A. Thomas, J. A. Hutchison, E. Devaux, C. Genet, and T. W. Ebbesen, Non-radiative energy transfer mediated by hybrid light-matter states, *Angewandte Chemie International Edition* **55**, 6202 (2016).
- [16] J. Schachenmayer, C. Genes, E. Tignone, and G. Pupillo, Cavity-enhanced transport of excitons, *Phys. Rev. Lett.* **114**, 196403 (2015).
- [17] F. Herrera and F. C. Spano, Cavity-controlled chemistry in molecular ensembles, *Phys. Rev. Lett.* **116**, 238301 (2016).
- [18] C. Schäfer, M. Ruggenthaler, H. Appel, and A. Rubio, Modification of excitation and charge transfer in cavity quantum-electrodynamical chemistry, *Proceedings of the National Academy of Sciences* **116**, 4883 (2019).
- [19] J. A. Campos-Gonzalez-Angulo, R. F. Ribeiro, and J. Yuen-Zhou, Resonant catalysis of thermally activated chemical reactions with vibrational polaritons, *Nature Communications* **10**, 1 (2019).
- [20] T. E. Li, A. Nitzan, and J. E. Subotnik, Collective vibrational strong coupling effects on molecular vibrational relaxation and energy transfer: Numerical insights via cavity molecular dynamics simulations, *Angewandte Chemie International Edition* **60**, 15533 (2021).
- [21] D. Wang, H. Kelkar, D. Martin-Cano, T. Utikal, S. Göttinger, and V. Sandoghdar, Coherent coupling of

- a single molecule to a scanning fabry-perot microcavity, *Phys. Rev. X* **7**, 021014 (2017).
- [22] O. S. Ojambati, R. Chikkaraddy, W. D. Deacon, M. Horton, D. Kos, V. A. Turek, U. F. Keyser, and J. J. Baumberg, Quantum electrodynamics at room temperature coupling a single vibrating molecule with a plasmonic nanocavity, *Nature Communications* **10**, 10.1038/s41467-019-08611-5 (2019).
- [23] J. Flick, M. Ruggenthaler, H. Appel, and A. Rubio, Atoms and molecules in cavities, from weak to strong coupling in quantum-electrodynamics (qed) chemistry, *Proceedings of the National Academy of Sciences* **114**, 3026 (2017).
- [24] T. S. Haugland, E. Ronca, E. F. Kjønstad, A. Rubio, and H. Koch, Coupled cluster theory for molecular polaritons: Changing ground and excited states, *Physical Review X* **10**, 041043 (2020).
- [25] E. Peter, P. Senellart, D. Martrou, A. Lemaitre, J. Hours, J. Gérard, and J. Bloch, Exciton-photon strong-coupling regime for a single quantum dot embedded in a microcavity, *Physical review letters* **95**, 067401 (2005).
- [26] X. Liu, T. Galfsky, Z. Sun, F. Xia, E.-c. Lin, Y.-H. Lee, S. Kéna-Cohen, and V. M. Menon, Strong light-matter coupling in two-dimensional atomic crystals, *Nature Photonics* **9**, 30 (2015).
- [27] S. Latini, D. Shin, S. A. Sato, C. Schäfer, U. De Giovannini, H. Hübener, and A. Rubio, The ferroelectric photo ground state of SrTiO₃: Cavity materials engineering, *Proceedings of the National Academy of Sciences* **118** (2021).
- [28] A. Thomas, J. George, A. Shalabney, M. Dryzhakov, S. J. Varma, J. Moran, T. Chervy, X. Zhong, E. Devaux, C. Genet, J. A. Hutchison, and T. W. Ebbesen, Ground-state chemical reactivity under vibrational coupling to the vacuum electromagnetic field, *Angewandte Chemie International Edition* **55**, 11462 (2016).
- [29] A. Thomas, A. Jayachandran, L. Lethuillier-Karl, R. M. Vergauwe, K. Nagarajan, E. Devaux, C. Genet, J. Moran, and T. W. Ebbesen, Ground state chemistry under vibrational strong coupling: dependence of thermodynamic parameters on the rabi splitting energy, *Nanophotonics* **9**, 249 (2020).
- [30] W. Ahn, F. Herrera, and B. Simpkins, Modification of urethane addition reaction via vibrational strong coupling, *ChemRxiv* 10.26434/chemrxiv-2022-wb6vs (2022).
- [31] A. Thomas, L. Lethuillier-Karl, K. Nagarajan, R. M. A. Vergauwe, J. George, T. Chervy, A. Shalabney, E. Devaux, C. Genet, J. Moran, and T. W. Ebbesen, Tilting a ground-state reactivity landscape by vibrational strong coupling, *Science* **363**, 615 (2019).
- [32] J. Lather, P. Bhatt, A. Thomas, T. W. Ebbesen, and J. George, Cavity catalysis by cooperative vibrational strong coupling of reactant and solvent molecules, *Angewandte Chemie International Edition* **58**, 10635 (2019).
- [33] J. Galego, C. Climent, F. J. Garcia-Vidal, and J. Feist, Cavity casimir-polder forces and their effects in ground-state chemical reactivity, *Physical Review X* **9**, 021057 (2019).
- [34] J. A. Campos-Gonzalez-Angulo and J. Yuen-Zhou, Polaritonic normal modes in transition state theory, *The Journal of chemical physics* **152**, 161101 (2020).
- [35] T. E. Li, A. Nitzan, and J. E. Subotnik, On the origin of ground-state vacuum-field catalysis: Equilibrium consideration, *The Journal of Chemical Physics* **152**, 234107 (2020).
- [36] X. Li, A. Mandal, and P. Huo, Cavity frequency-dependent theory for vibrational polariton chemistry, *Nature Communications* **12**, 10.1038/s41467-021-21610-9 (2021).
- [37] C. Climent and J. Feist, On the SN2 reactions modified in vibrational strong coupling experiments: reaction mechanisms and vibrational mode assignments, *Physical Chemistry Chemical Physics* **22**, 23545 (2020).
- [38] A. Thomas, L. Lethuillier-Karl, J. Moran, and T. Ebbesen, Comment on on the SN2 reactions modified in vibrational strong coupling experiments: Reaction mechanisms and vibrational mode assignments (2020), *ChemRxiv:12982358.v1*.
- [39] M. Ruggenthaler, J. Flick, C. Pellegrini, H. Appel, I. V. Tokatly, and A. Rubio, Quantum-electrodynamical density-functional theory: Bridging quantum optics and electronic-structure theory, *Phys. Rev. A* **90**, 012508 (2014).
- [40] J. Flick and P. Narang, Cavity-correlated electron-nuclear dynamics from first principles, *Phys. Rev. Lett.* **121**, 113002 (2018).
- [41] C. Schäfer, F. Buchholz, M. Penz, M. Ruggenthaler, and A. Rubio, Making ab initio qed functional (s): Non-perturbative and photon-free effective frameworks for strong light-matter coupling, *Proceedings of the National Academy of Sciences* **118** (2021).
- [42] V. R. Chintareddy, K. Wadhwa, and J. G. Verkade, Tetrabutylammonium fluoride (tba^f)–catalyzed addition of substituted trialkylsilylalkynes to aldehydes, ketones, and trifluoromethyl ketones, *The Journal of organic chemistry* **76**, 4482 (2011).
- [43] C. Schäfer, M. Ruggenthaler, V. Rokaj, and A. Rubio, Relevance of the quadratic diamagnetic and self-polarization terms in cavity quantum electrodynamics, *ACS photonics* **7**, 975 (2020).
- [44] Y. Pang, A. Thomas, K. Nagarajan, R. M. Vergauwe, K. Joseph, B. Patraha, K. Wang, C. Genet, and T. W. Ebbesen, On the role of symmetry in vibrational strong coupling: the case of charge-transfer complexation, *Angewandte Chemie* **132**, 10522 (2020).
- [45] S. Schütz, J. Schachenmayer, D. Hagenmüller, G. K. Brennen, T. Volz, V. Sandoghdar, T. W. Ebbesen, C. Genes, and G. Pupillo, Ensemble-induced strong light-matter coupling of a single quantum emitter, *Physical review letters* **124**, 113602 (2020).
- [46] D. Siedler, C. Schäfer, M. Ruggenthaler, and A. Rubio, Polaritonic chemistry: Collective strong coupling implies strong local modification of chemical properties, *The Journal of Physical Chemistry Letters* **12**, 508 (2020).
- [47] F. Neese, Software update: the orca program system, version 4.0, *WIREs Computational Molecular Science* **8**, e1327 (2018).
- [48] N. Tancogne-Dejean, M. J. Oliveira, X. Andrade, H. Appel, C. H. Borca, G. Le Breton, F. Buchholz, A. Castro, S. Corni, A. A. Correa, *et al.*, Octopus, a computational framework for exploring light-driven phenomena and quantum dynamics in extended and finite systems, *The Journal of chemical physics* **152**, 124119 (2020).
- [49] C. Schäfer, M. Ruggenthaler, and A. Rubio, Ab initio nonrelativistic quantum electrodynamics: Bridging quantum chemistry and quantum optics from weak to strong coupling, *Physical Review A* **98**, 043801 (2018).

- [50] X. Andrade, A. Castro, D. Zueco, J. Alonso, P. Echenique, F. Falceto, and A. Rubio, Modified ehrenfest formalism for efficient large-scale ab initio molecular dynamics, *Journal of chemical theory and computation* **5**, 728 (2009).
- [51] J. Perdew, K. Burke, and M. Ernzerhof, Perdew, burke, and ernzerhof reply, *Physical Review Letters* **80**, 891 (1998).

ACKNOWLEDGMENTS

We thank Anoop Thomas, Michael Ruggenthaler, and Göran Johansson for insightful discussions. The Flatiron Institute is a division of the Simons Foundation.

Funding

This work was supported by the European Research Council (ERC-2015-AdG694097), the Cluster of Excellence 'CUI: Advanced Imaging of Matter' of the Deutsche Forschungsgemeinschaft (DFG) - EXC 2056 - project ID 390715994, Grupos Consolidados (IT1249-19), partially by the Federal Ministry of Education and Research Grant RouTe-13N14839, the SFB925 "Light induced dynamics and control of correlated quantum systems", the Swedish Research Council (VR) through Grant No. 2016-06059, the Department of Energy, Photonics at Thermo-

dynamic Limits Energy Frontier Research Center, under Grant No. DE-SC0019140. P.N. gratefully acknowledges a Moore Inventor Fellowship through Grant GBMF8048 from the Gordon and Betty Moore Foundation and support from the CIFAR BSE Program's 'Catalyst' grant.

Author Contributions

C.S., J.F., and E.R. contributed equally. A.R. and C.S. conceived the project. C.S., J.F., and E.R. obtained, evaluated and interpreted the data. C.S. prepared a first draft, C.S. and E.R. prepared the figures with input from all authors. All authors discussed the results and edited the manuscript.

Competing interests

None

Data and materials availability

Data and scripts can be obtained from the authors upon reasonable request. The numerical implementation is part of the development branch of the Octopus code.

Supplemental Information to: Shining Light on the Microscopic Resonant Mechanism Responsible for Cavity-Mediated Chemical Reactivity

Christian Schäfer,^{1,2,3,4,*} Johannes Flick,^{5,6,†} Enrico Ronca,^{7,‡} Prineha Narang,^{6,§} and Angel Rubio^{1,2,5,¶}

¹Max Planck Institute for the Structure and Dynamics of Matter and
Center for Free-Electron Laser Science & Department of Physics,
Luruper Chaussee 149, 22761 Hamburg, Germany

²The Hamburg Center for Ultrafast Imaging, Luruper Chaussee 149, 22761 Hamburg, Germany

³Department of Physics, Chalmers University of Technology, 412 96 Göteborg, Sweden

⁴Department of Microtechnology and Nanoscience, MC2,
Chalmers University of Technology, 412 96 Göteborg, Sweden

⁵Center for Computational Quantum Physics, Flatiron Institute, 162 5th Ave., New York, 10010 NY, USA

⁶John A. Paulson School of Engineering and Applied Sciences,
Harvard University, Cambridge, Massachusetts 02138, USA

⁷Istituto per i Processi Chimico Fisici del CNR (IPCF-CNR), Via G. Moruzzi, 1, 56124, Pisa, Italy

(Dated: May 26, 2022)

I. DISCUSSION OF THE VIBRATIONAL MODES, ENERGETICS, FUNCTIONAL AND SOLVENT EFFECTS

Fig. S1 illustrates the vibrational spectrum including the PTA+F⁻ initial state and an intermediate strongly stretched state. During the evolution of the reaction, the vibrational modes are constantly changing which allows many more frequencies to dynamically couple to the cavity than the equilibrium PTA or PTAF⁻ structures would suggest. The dynamic shift of the vibrational mode during the reaction could contribute to broadened resonances.

The vibro-polaritonic spectrum in direction of polarization for different light-matter coupling strength is plotted in fig. S2. The results are comparable to fig. 1 in the main manuscript but utilize the finite-difference Born-Oppenheimer approach outlined in [1]. For large light-matter coupling (as used in fig. 4), the R^2 self-polarization term (black dashed-dotted) leads to a sizeable blue-shift of the excitation. Comparison with fig. 4 (b) suggests that this effect is responsible for the observed blue-shift with increasing frequency as we keep $g_0/\hbar\omega$ constant. Finite-difference and time-dependent vibrational linear response calculations are slightly shifted with respect to each other.

The here chosen semi-classical treatment of light does not change the ground-state potential energy-surface itself but can merely affect the dynamic of the system. Surely, (ultra-)strong light-matter coupling will lead to correlated ground-states comprising electronic, nuclear and photonic degrees of freedom. It has been shown, that

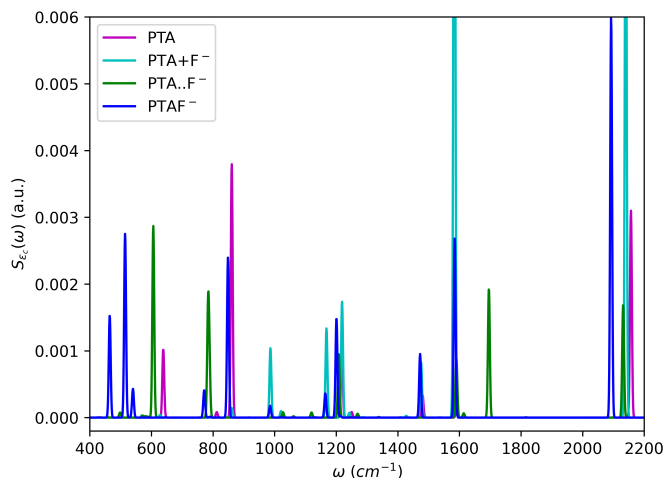


FIG. 1. Vibrational absorption spectrum along the cavity polarization direction $S_{\epsilon_c}(\omega) = 2\omega \sum_{j=1}^{N_{vib}} |\epsilon_c \cdot \mathbf{R}(\omega_j)|^2 \delta(\omega - \omega_j)$ for the bare PTA complex (magenta), our initial state PTA+F⁻ (cyan), an intermediate state with strongly stretched Si-F bond of 2.889 Å (green), and the pentavalent PTAF⁻ complex (blue). Vibrational resonances are artificially broadened. In agreement with fig. 1 (d), the polarization of the coupled cavity mode is aligned along the Si-C axis. This linear response calculation used the default normalization implemented in Octopus while all other used a new normalization.

already this path allows strong light-matter coupling to influence electronic structure and thus chemistry [2–7]. In the present work, calculations using the KLI functional [5] suggested very small modifications of the electronic structure when strongly coupled to the cavity.

In order to eliminate the possibility that the solvent is an integral component of the mechanism that is put forward here, we used ORCA with a continuous PCM model description for the solvent methanol. We obtain the energetic values for reactant [PTA+F] = -816.131244 *H*, pentavalent complex [PTAF]⁻ = -816.1943141865 *H*, transition-state [PA ... Me3SiF] = -816.18146281 *H* and

* Electronic address: christian.schaefer.physics@gmail.com

† Electronic address: jflick@flatironinstitute.org

‡ Electronic address: enrico.ronca@pi.ipcf.cnr.it

§ Electronic address: prineha@seas.harvard.edu

¶ Electronic address: angel.rubio@mpsd.mpg.de

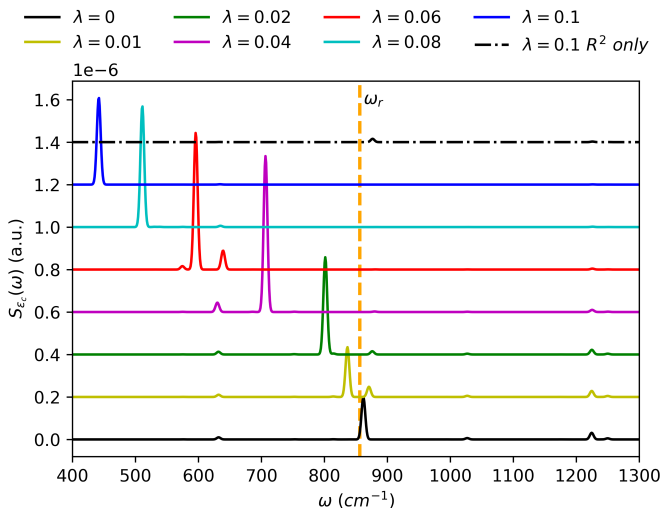


FIG. 2. Vibro-polaritonic absorption spectrum along the cavity polarization direction $S_{\epsilon_c}(\omega) = 2\omega \sum_{j=1}^{N_{vib}} |\epsilon_c \cdot \mathbf{R}(\omega_j)|^2 \delta(\omega - \omega_j)$ for the PTA complex coupled to a cavity mode with increasing coupling strength λ [a.u.]. The orange-dashed vertical line indicates the selected cavity frequency. The black-dashed curve represents the PTA spectrum when affected by the self-polarization term of the cavity only, i.e., no bilinear coupling is included. The value of $\lambda = 0.1$ a.u. corresponds to $g_0/\hbar\omega_c = 1.132$.

product [PA- + Me3SiF] = -816.1846728 H . We obtain an enthalpy between pentavalent complex and transition-state of $\Delta H^\ddagger \approx 0.35$ eV ≈ 34 kJ/mol in good agreement with experimental results (30 and 39 kJ/mol) [8, 9]. Ignoring entropic features as well as bond termination with hydrogen, the resulting product is higher in energy than the intermediate step. The experimental investigations suggest that the entropic barrier (54 kJ/mol) is non-negligible. In our simulations, this is expressed in the very narrow window of initial configurations that result in F attaching to PTA and subsequent bond breaking. Thus, the likelihood of the reaction taking place is largely determined by the unlikeliness of a specific initial configuration in addition to the energetic barrier that describes the bond breaking.

We estimated if our observations depend critically on the exchange-correlation potential in two ways. First, by calculating the Si-C C=C potential energy surface for the 60% configuration in ORCA using two different basis sets and two different functionals (see fig. S3). While quantitative changes can be observed, they agree qualitatively such that our observations are likely to be robust against changing basis-set or DFT-functional.

Second, by calculating in ORCA the vibrational spectrum and the corresponding Si-C stretching contribution for different levels of theoretical description, shown in fig. S4. The positions of vibrational excitations and their Si-C stretching contribution is only marginally affected by the choice of functional, solvent or basis. Noticeable differences appear however in the relative spectral strength (especially around 300, 500 and 2000 cm^{-1}).

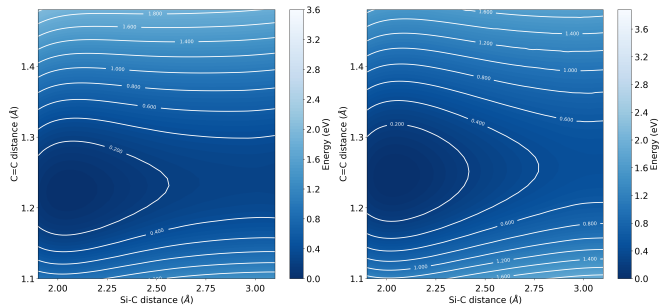


FIG. 3. Si-C C=C potential energy surface calculated with ORCA (F out of Si-C axis). Left, using the B3LYP functional and the def2-TZVP basis, right, using the PBE functional and the 6-31G* basis.

In conclusion, our theoretical QEDFT calculations presented in the main text can be expected to provide a good description of the energetics and a qualitative description of the relevant mechanism. While our calculations suggest indeed a comparably small Si-C character in the experimentally coupled vibration, in agreement with [10], it seems as if the Si-C weighted spectrum provides a more reliable measure for the cavity influence on the reactivity. Fig. S4 indicates that especially the relative spectral strength is a sensitive quantity for which the theoretical calculations must be considered of limited reliability.

II. MODE PROJECTION AT 570 CM^{-1}

We elaborated in the main text that coupling strongly to vibrations around $\omega_c = 570$ cm^{-1} leads to a particularly strong influence on the chemical reactivity. Fig. S5 illustrates the corresponding mode-projection, equivalent to fig. 3 in the main text. In comparison with fig. 3, the vibration at 771 cm^{-1} is now less affected and the dominant effect of the resonant cavity is an accumulation of occupation around 500 cm^{-1} .

III. BOND CORRELATION

Intuitively, energy redistribution between vibrations suggests (classical) correlation among them. If we assume that specific bonds are particularly characteristic for the involved vibrations, we might want to investigate to which extent those local bonds are correlated among each other. This would provide an intuitive understanding of the anharmonic couplings and local changes due to the cavity. Fig. S6 illustrates the classical bond correlation among a few most characteristic bonds in the F-Si-C=C-Benzene chain of PTAF⁻. While minor changes in the correlation between Si-C and Si-F bond indicate that the F-Si-Meth complex undergoes vibrational changes depending on the resonant condition, those changes are small and do not allow to draw a clear conclusion.

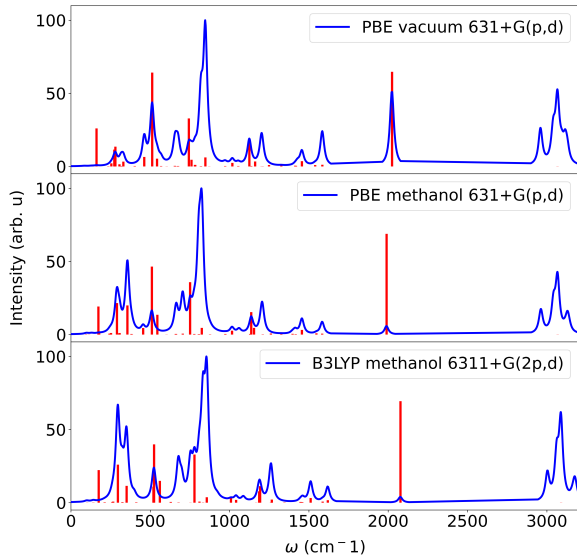


FIG. 4. Vibrational spectrum along a polarization aligned with the Si-C axis for different functionals, solvents and basis-sets. The spectra are obtained with ORCA using an artificial broadening of 30 cm^{-1} and the Si-C-stretching contributions are multiplied by 150 for better visibility. While energetic positions are largely insensitive to functional, solvent and basis, clear deviations in the relative spectral intensity become apparent. Our QEDFT calculations use a finite-difference grid, the PBE functional and vacuum.

IV. CURVATURE AT THE TRANSITION-STATE AND RESONANT FREQUENCIES

Li et al. [11] suggested recently that the resonant effect of the slow down of a reaction under vibrational strong coupling originates from an effective solvent-caging effect around the transition-state. Thereby, the suggested resonant frequency emerges from the curvature of the PES at the transition-state $M\omega_b^2 = -\partial_R^2 E|_{TS}$. This would lead to a resonant frequency at $\omega = 74 \text{ cm}^{-1}$ [11]. We observe a clear resonance in the reactivity at $\omega = 86 \text{ cm}^{-1}$ which corresponds quite accurately to the transition-state curvature without solvent and the chosen PBE functional (Table I). Furthermore, we obtain multiple additional resonances when the cavity is close to vibrations with substantial Si-C character, including the experimental resonance at 860 cm^{-1} . This suggests that both mechanisms, i.e., dynamical caging and vibrational energy redistribution, provide possible mechanism at the single-molecule strong-coupling level.

Table I presents the binding frequency (lowest imaginary vibrational frequency at the transition-state) calculated with ORCA for different solvents, Gaussian basis-sets, and relative orientations of the F anion with respect to the Si-C bond-axis.

Theory level	Solvent	F position	ω_b [cm^{-1}]
PBE 6-31G*	Vacuum	in-axis	90
PBE 6-31G*	Methanol	in-axis	94
PBE 6-311G*	Methanol	in-axis	88
B3LYP 6-31G*	Methanol	in-axis	93
PBE 6-31G*	Acetonitrile	in-axis	94
PBE 6-31G*	Vacuum	off-axis	85
PBE 6-311G*	Methanol	off-axis	81
Li et al. [11]	Methanol	in-axis	74
			Resonance [cm^{-1}]
QEDFT (PBE)	Vacuum	in-axis	≈ 86
			≈ 292
			≈ 515
			≈ 771
			≈ 849
			≈ 1201
Experiment [8]	Methanol	-	860
Related exp. [12]	Methanol	-	1250

TABLE I. Lowest (imaginary) vibrational frequency at the transition-state for the two different configurations calculated with different solvents and theoretical descriptions. The QEDFT calculations capture the dynamical caging effect around the binding frequency in addition to the other resonances at vibrational frequencies with strong Si-C character. We decided to label the QEDFT resonances by the associated vibrational excitations, our time-dependent calculations suggest an increasing blue-shift for increasing frequency. The available experiments [8, 9] suggests a resonance at 860 cm^{-1} and a related experiment at 1250 cm^{-1} [12].

A. Coupling strength dependence of the cavity mediated influence on chemical reactivity

As illustrated in fig. S7, increasing light-matter coupling strength will lead to an increase of the cavity influence on the chemical reactivity. The shown trend is consistent with the rate-change measured in experiment (compare to fig. 3 a in [8], Rabi-splitting is $\propto g_0/\hbar\omega_c$). Although our single-particle coupling strength is considerably larger than in experiment, the cavity has to influence the reactive trajectory within a much shorter time in our calculations such that larger couplings are necessary for noticeable influence. The short reaction-time in our calculations originates from the selection of favourable initial states, representing a very small subset of the full statistical ensemble of all possible initial states.

B. Preventing the Attachment of F^-

When we increase the light-matter coupling strength, two distinct effects can be observed. First, the inhibition

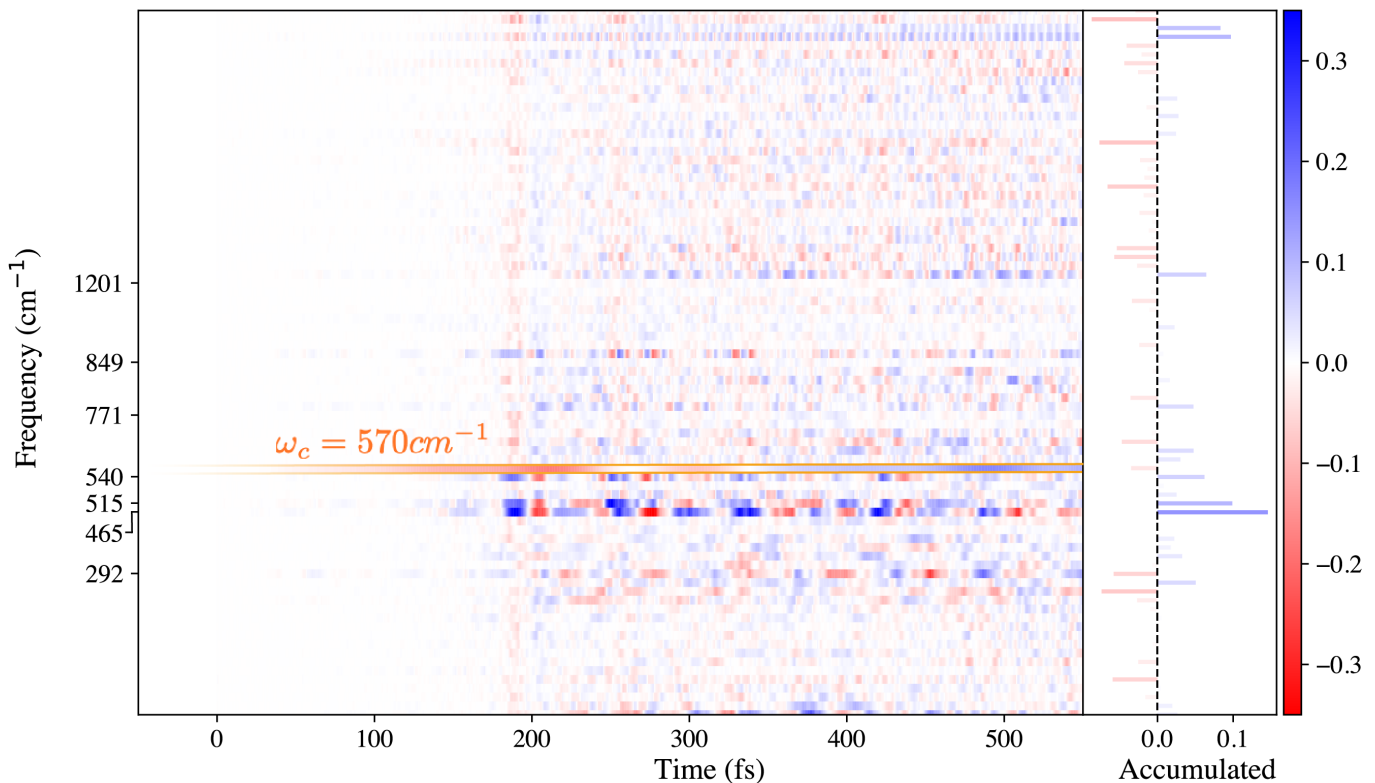


FIG. 5. Time-resolved influence on the mode occupations by resonant vibrational strong-coupling. Illustrated is the trajectory averaged difference in normalized mode-occupation between $\omega_c = 570 \text{ cm}^{-1}$, $g_0/\hbar\omega_c = 1.132$ and far off-resonance $\omega_c = 43 \text{ cm}^{-1}$, $g_0/\hbar\omega_c = 1.132$ for all 8 trajectories that undergo the reaction outside the cavity. The bar-plot shows the accumulated difference divided by a factor 100. The cavity mode (bordered orange) is here represented by the difference in normalized mode-displacement $q(t) = \sqrt{\hbar/2\omega_c}(\hat{a}^\dagger + \hat{a})$ and re-scaled by the factor $1/4$.

of the chemical reaction intensifies, that is, more trajectories will be stronger affected, second the approach of the F^- anion is delayed. Fig. S8 presents the forces acting on F projected on the cavity polarization axis for increasing light-matter coupling. During the dynamical approach of the F^- to the PTA complex, the methyl groups of the PTA complex need to rearrange to provide space for F^- . This leads to a short repellent force acting during the rearrangement time. The approaching F^- induces noticeable changes in the molecular dipole moment, resulting in an effective nuclear current coupling to the photonic system.

With increasing coupling strength, the latter results in an increasing repulsion which partially prevents F^- from attaching to PTA. The dynamic change of the molecular dipole with approaching F^- results therefore in an additional reaction-barrier. Considering that the reaction probability is slim in the first place, the success of F^- attacking and subsequently the rate of reactions is sensitive to any alternation of the F^- trajectory. This observation provides another possible explanation for the experimentally obtained large entropic change in the reaction character [8, 9] but would not feature the same dependence on the resonant condition as observed in the main paper and is comparably weak.

V. DELAY OF REACTION WITHOUT PREVENTION

The majority of the trajectories undergoing the reaction far off-resonant or in free-space no longer show a reactive behaviour close to any of the discussed resonances. For all of those cases, the trajectory is trapped close to the local minimum at the pentavalent PTA complex, potentially stretching the Si-C bond but relaxing back to the local minimum. Single trajectories can however undergo the reaction at longer times as fig. S9 illustrates. As the statistical ensemble becomes increasingly insufficient the longer the time-propagation, we decide to limit the presentation of the resonant effect to the first 700 fs. If we would select a much smaller coupling strength, the influence of the cavity would be also substantially smaller, i.e., many of the aforementioned trajectories close to resonance would resemble closer those off-resonance. One should note hereby that the reaction is unlikely to happen from the start, our ensemble is already sampled around the ideal initial state which leads to the quick reaction speed of ps compared to the minutes of acquisition in experiment. This implies, that a much larger ensemble and a much longer propagation time would be needed to resolve the reaction and its changes if we would not select

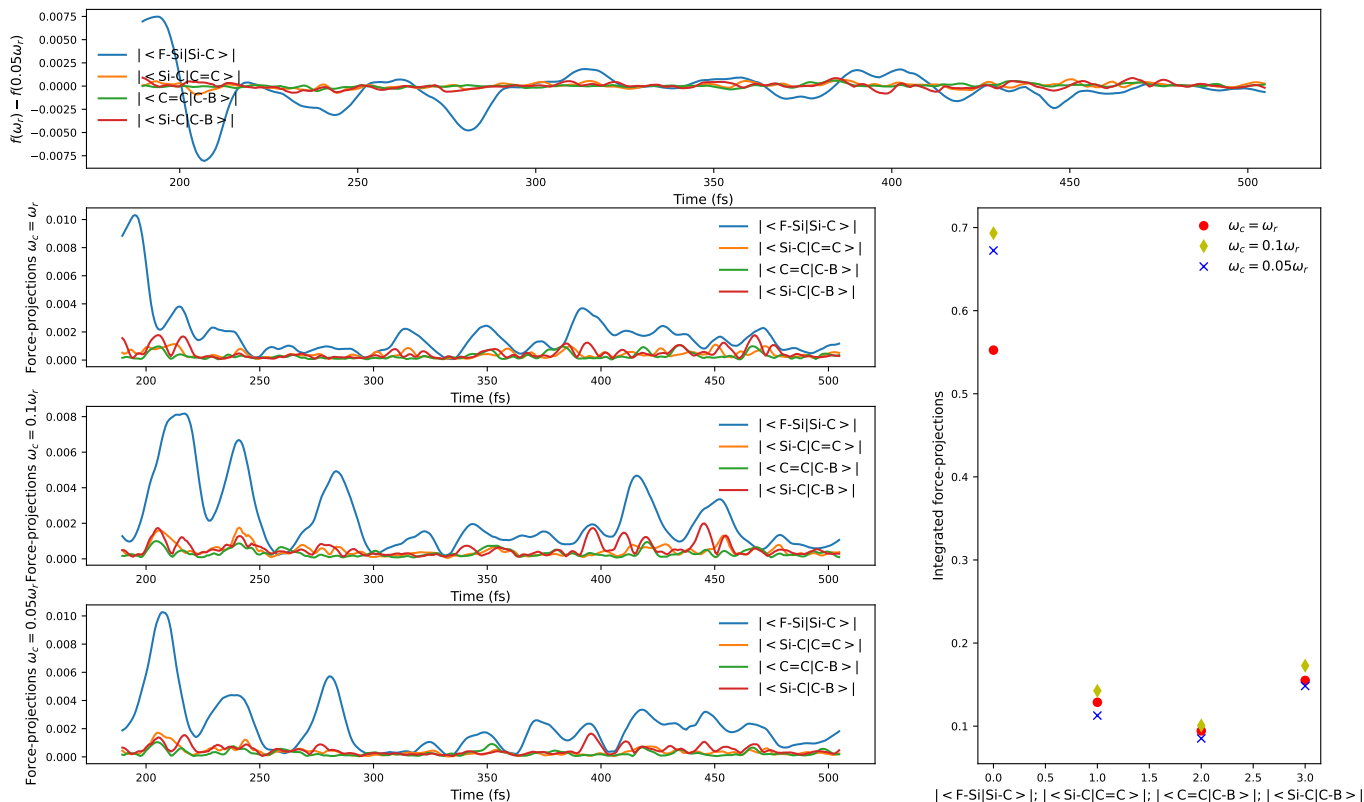


FIG. 6. Classical bond correlations for resonant ($\omega_r = 856$, 2nd row, left), lowest frequency (bottom, left), their difference (top), their integrated values (right) and the bond correlations for the dynamical caging resonance (3rd row, left). Calculated are the projections of the forces acting on the individual bonds, i.e., the classical time-dependent correlation between the forces acting on Si-C and Si-F bond (blue) are for instance $|\langle f_{Si} - f_C | f_{Si} - f_F \rangle|$ which provides an estimate for how strong deformation of the Si-C bond influences deformation of the Si-F bond and vice versa. C-B denotes hereby the Carbon-Benzene bond and C=C the Carbon triple bond located between the Si-C functional group and the C-B bond. We see small differences in the Si-F Si-C bond correlations between the resonant and off-resonant situation. This might indicate that other bonds are substantially contributing in the cavity mediated energy redistribution (e.g. the Si-methyl bonds) but foremost clarifies that the Si-C bond is distributed over various vibrations. Future investigations could try to localize the vibrational modes (local vibrational mode basis) in order to better identify local changes that influence the Si-C bond breaking as a consequence of the resonant condition.

such a strong light-matter strength and preferable initial

state. Consequently, the present computational limitations advice the here presented approach.

-
- [1] J. Bonini and J. Flick, Ab initio linear-response approach to vibro-polaritons in the cavity born–oppenheimer approximation, *Journal of Chemical Theory and Computation* **18**, 2764 (2022), pMID: 35404591, <https://doi.org/10.1021/acs.jctc.1c01035>.
- [2] C. Schäfer, M. Ruggenthaler, H. Appel, and A. Rubio, Modification of excitation and charge transfer in cavity quantum-electrodynamical chemistry, *Proceedings of the National Academy of Sciences* **116**, 4883 (2019).
- [3] C. Schäfer, F. Buchholz, M. Penz, M. Ruggenthaler, and A. Rubio, Making ab initio qed functional (s): Non-perturbative and photon-free effective frameworks for strong light–matter coupling, *Proceedings of the National Academy of Sciences* **118** (2021).
- [4] J. Flick, M. Ruggenthaler, H. Appel, and A. Rubio, Atoms and molecules in cavities, from weak to strong coupling in quantum-electrodynamics (qed) chemistry, *Proceedings of the National Academy of Sciences* **114**, 3026 (2017).
- [5] J. Flick, C. Schäfer, M. Ruggenthaler, H. Appel, and A. Rubio, Ab initio optimized effective potentials for real molecules in optical cavities: Photon contributions to the molecular ground state, *ACS Photonics* **5**, 992 (2018), <https://doi.org/10.1021/acsphotonics.7b01279>.
- [6] T. S. Haugland, E. Ronca, E. F. Kjønsstad, A. Rubio, and H. Koch, Coupled cluster theory for molecular polaritons: Changing ground and excited states, *Physical Review X* **10**, 041043 (2020).
- [7] T. S. Haugland, C. Schäfer, E. Ronca, A. Rubio, and H. Koch, Intermolecular interactions in optical cavities: An ab initio qed study, *The Journal of Chemical Physics* **154**, 094113 (2021).

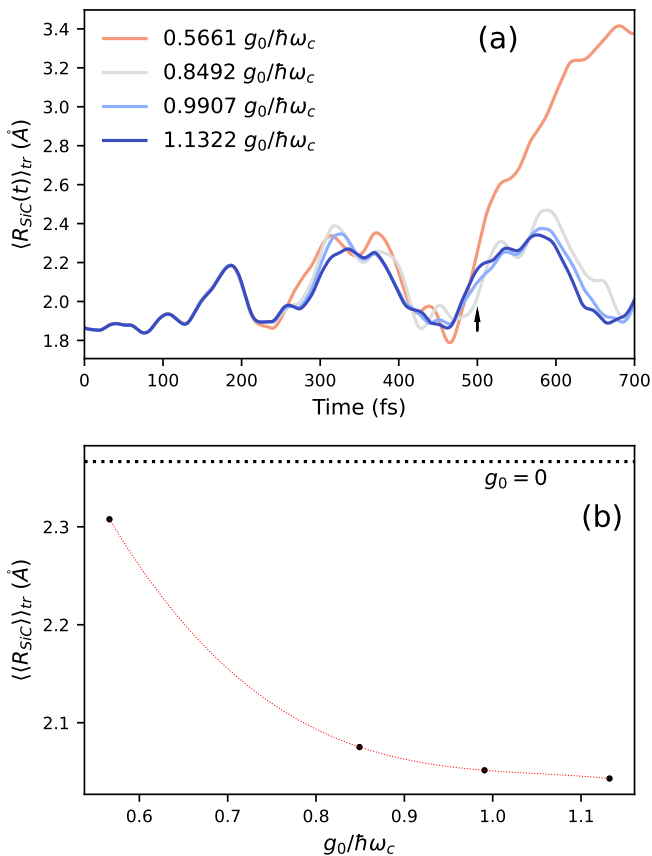


FIG. 7. Time-resolved trajectory averaged Si-C distance (a) and time-averaged Si-C distance $\langle \langle R_{SiC} \rangle \rangle_{tr}$ (b) for cavity frequency $\omega_c = 571 \text{ cm}^{-1}$. The ratio $g_0/\hbar\omega_c$ is varied, the red-dotted line represents a cubic spline interpolation and serves as guide to the eye. We use all 8 trajectories that show the reaction outside the cavity.

[8] A. Thomas, J. George, A. Shalabney, M. Dryzhakov, S. J. Varma, J. Moran, T. Chervy, X. Zhong, E. Devaux, C. Genet, J. A. Hutchison, and T. W. Ebbesen, Ground-state chemical reactivity under vibrational coupling to

the vacuum electromagnetic field, *Angewandte Chemie International Edition* **55**, 11462 (2016).

- [9] A. Thomas, A. Jayachandran, L. Lethuillier-Karl, R. M. Vergauwe, K. Nagarajan, E. Devaux, C. Genet, J. Moran, and T. W. Ebbesen, Ground state chemistry under vibrational strong coupling: dependence of thermodynamic parameters on the rabi splitting energy, *Nanophotonics* **9**, 249 (2020).
- [10] C. Climent and J. Feist, On the SN2 reactions modified in vibrational strong coupling experiments: reaction mechanisms and vibrational mode assignments, *Physical Chemistry Chemical Physics* **22**, 23545 (2020).
- [11] X. Li, A. Mandal, and P. Huo, Cavity frequency-dependent theory for vibrational polariton chemistry, *Nature Communications* **12**, 10.1038/s41467-021-21610-9 (2021).
- [12] A. Thomas, L. Lethuillier-Karl, K. Nagarajan, R. M. A. Vergauwe, J. George, T. Chervy, A. Shalabney, E. Devaux, C. Genet, J. Moran, and T. W. Ebbesen, Tilting a ground-state reactivity landscape by vibrational strong

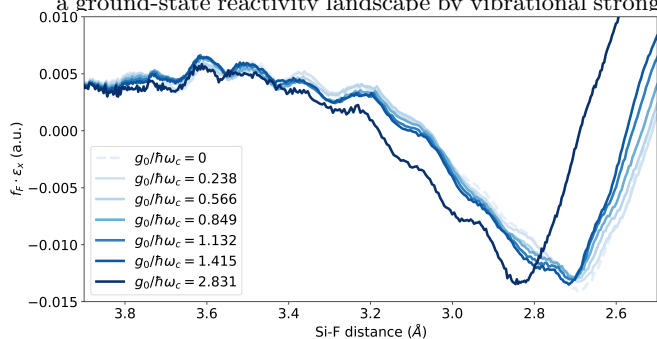


FIG. 8. Force acting on the F atom along the cavity polarization axis for the trajectory corresponding to fig. 2 (resonant). With increasing light-matter coupling a weak repellent force is induced that prevents the F anion to attack the PTA complex. The Ehrenfest light-matter coupling utilized here becomes less reliable for larger coupling strength, the overall strength of the effect can be expected to be weak for experimental values.

coupling, *Science* **363**, 615 (2019).

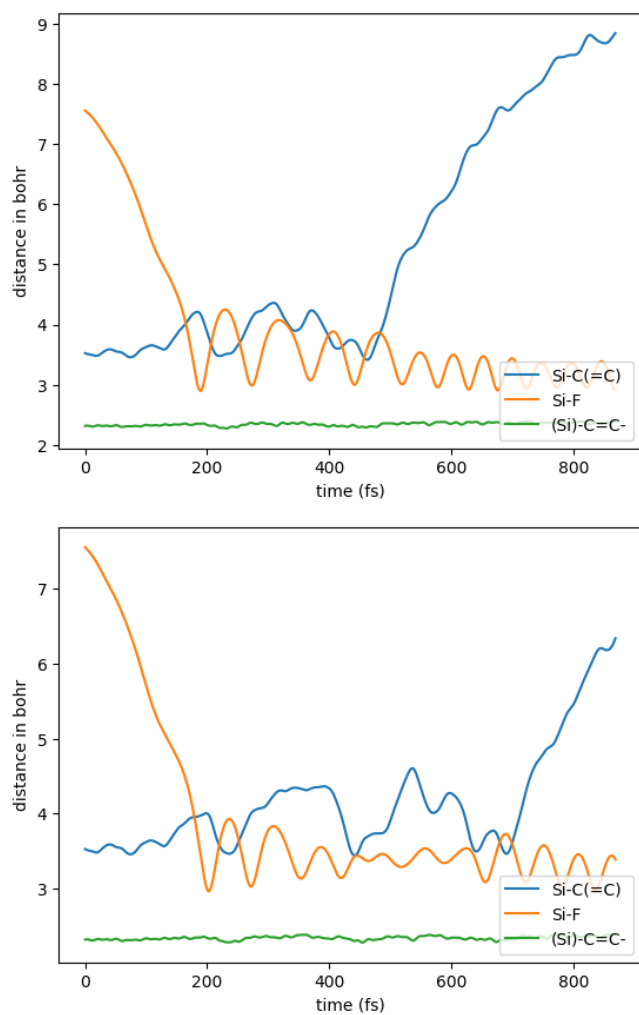


FIG. 9. Time-dependent bond distances in free-space (top) and at $\omega_c = 86 \text{ cm}^{-1}$ (bottom). The Si-C bond (blue) crosses the transition-state at around 500 fs in free-space and at 800 fs around the dynamical caging frequency.